Cell

RIPK1 Regulates RIPK3-MLKL-Driven Systemic Inflammation and Emergency Hematopoiesis

James A. Rickard,[1,2,9] Joanne A. O'Donnell,[1,2,9] Joseph M. Evans,[1,3,9] Najoua Lalaoui,[1,2] Ashleigh R. Poh,[1,2] TeWhiti Rogers,[4] James E. Vince,[1,2] Kate E. Lawlor,[1,2] Robert L. Ninnis,[1,2] Holly Anderton,[1,2] Cathrine Hall,[1,2] Sukhdeep K. Spall,[1,2] Toby J. Phesse,[1,2] Helen E. Abud,[5] Louise H. Cengia,[1,2] Jason Corbin,[1,2] Sandra Mifsud,[1,2] Ladina Di Rago,[1,2] Donald Metcalf,[1,2] Matthias Ernst,[1,2] Grant Dewson,[1,2] Andrew W. Roberts,[1,2,6] Warren S. Alexander,[1,2] James M. Murphy,[1,2] Paul G. Ekert,[1,2] Seth L. Masters,[1,2] David L. Vaux,[1,2] Ben A. Croker,[1,2,7,10] Motti Gerlic,[1,2,8,10,*] and John Silke[1,2,10,*]

[1]The Walter and Eliza Hall Institute of Medical Research, Parkville, VIC 3052, Australia
[2]Department of Medical Biology, University of Melbourne, Parkville, VIC 3050, Australia
[3]Department of Biochemistry, La Trobe University, Bundoora, VIC 3086, Australia
[4]Department of Pathology, University of Melbourne, Parkville, VIC 3050, Australia
[5]Department of Anatomy and Developmental Biology, Monash University, Clayton, VIC 3800, Australia
[6]Faculty of Medicine, University of Melbourne, Parkville, VIC 3050, Australia
[7]Division of Hematology and Oncology, Boston Children's Hospital, Harvard Medical School, Boston, MA 02115, USA
[8]Department of Clinical Microbiology and Immunology, Sackler School of Medicine, Tel Aviv University, Tel Aviv 69978, Israel
[9]Co-first author
[10]Co-senior author
*Correspondence: mgerlic@post.tau.ac.il (M.G.), j.silke@latrobe.edu.au (J.S.)
http://dx.doi.org/10.1016/j.cell.2014.04.019

SUMMARY

Upon ligand binding, RIPK1 is recruited to tumor necrosis factor receptor superfamily (TNFRSF) and Toll-like receptor (TLR) complexes promoting prosurvival and inflammatory signaling. RIPK1 also directly regulates caspase-8-mediated apoptosis or, if caspase-8 activity is blocked, RIPK3-MLKL-dependent necroptosis. We show that C57BL/6 *Ripk1*$^{-/-}$ mice die at birth of systemic inflammation that was not transferable by the hematopoietic compartment. However, *Ripk1*$^{-/-}$ progenitors failed to engraft lethally irradiated hosts properly. Blocking TNF reversed this defect in emergency hematopoiesis but, surprisingly, *Tnfr1* deficiency did not prevent inflammation in *Ripk1*$^{-/-}$ neonates. Deletion of *Ripk3* or *Mlkl*, but not *Casp*8, prevented extracellular release of the necroptotic DAMP, IL-33, and reduced *Myd88*-dependent inflammation. Reduced inflammation in the *Ripk1*$^{-/-}$*Ripk3*$^{-/-}$, *Ripk1*$^{-/-}$*Mlkl*$^{-/-}$, and *Ripk1*$^{-/-}$*Myd88*$^{-/-}$ mice prevented neonatal lethality, but only *Ripk1*$^{-/-}$*Ripk3*$^{-/-}$*Casp8*$^{-/-}$ mice survived past weaning. These results reveal a key function for RIPK1 in inhibiting necroptosis and, thereby, a role in limiting, not only promoting, inflammation.

INTRODUCTION

Befitting its major inflammatory role, tumor necrosis factor (TNF) signaling via its receptor TNFR1 is highly regulated. In addition to driving the transcription of a host of inflammatory cytokines, TNF is also capable of initiating two cell death pathways, caspase-8-dependent apoptosis and RIPK1 kinase-dependent necroptosis (Vandenabeele et al., 2010). However, in the vast majority of cells, TNF does not induce cell death. It is believed that this is because the same IκB kinase (IKK)/mitogen-activated protein kinase (MAPK)-dependent increase in transcription that drives inflammatory cytokine production also upregulates antiapoptotic genes that inhibit the activation of caspase-8. Cellular FLICE-like inhibitory protein (cFLIP), a caspase-8 inhibitor, is chief among these antiapoptotic genes, and in the absence of cFLIP, TNF rapidly induces caspase-8-dependent apoptosis (Panayotova-Dimitrova et al., 2013; Piao et al., 2012). RIPK1 is believed to play an essential role in the activation of IKK/MAPK and in the transcription of cFLIP (Ea et al., 2006; Gentle et al., 2011; Micheau et al., 2001). In this role, it behaves as a structural element that is ubiquitylated by cellular inhibitor of apoptosis proteins (cIAPs) and linear ubiquitin chain assembly complex (LUBAC), and the ubiquitin chains decorating RIPK1 can recruit and trigger the activation of NF-κB and MAP kinases (Schmukle and Walczak, 2012; Wertz and Dixit, 2010). Consistent with an essential role for cFLIP in regulating caspase-8, *cFlip*/*Cflar* knockout mice die at embryonic stage E10.5 (Yeh et al., 2000).

Activation of caspase-8 by TNF occurs in a secondary cytoplasmic signaling complex that contains the protein Fas-associated protein with death domain (FADD) (Micheau and Tschopp, 2003). The death effector domain of FADD causes the oligomerization and autoactivation of caspase-8 (Wertz and Dixit, 2010). It is therefore surprising that *Fadd* and *Casp8* knockout mice both die at the same embryonic stage, from the same defects, as the *cFlip*/*Cflar*-deficient mice (Varfolomeev et al., 1998; Yeh et al., 1998). Because *Fadd*$^{-/-}$*Ripk3*$^{-/-}$ and *Casp8*$^{-/-}$*Ripk3*$^{-/-}$ mice

survive to adulthood (Kaiser et al., 2011; Oberst et al., 2011; Dillon et al., 2012), it is supposed that, in the absence of cFLIP, a lethal apoptotic pathway is initiated and that, in the absence of caspase-8 activation, an alternative lethal necroptotic RIPK1/RIPK3-dependent pathway occurs.

Therefore, current models for TNF signaling indicate that RIPK1 plays very important roles in two branches of the TNFR1 response: to inhibit apoptosis via cFLIP and to cause necroptosis in a RIPK1-kinase-dependent manner (Vandenabeele et al., 2010). Furthermore, RIPK1 may play similar roles in other innate immune signaling complexes, including Toll-like receptor (TLR) and MAVS/RIG-I (Kaiser et al., 2013; Meylan et al., 2004; Michallet et al., 2008). The pivotal role for RIPK1 in regulating outcomes from these innate immune signaling complexes makes the phenotype of the *Ripk1*$^{-/-}$ mice remarkable. In distinction to other regulators of the TNF pathway that die at embryonic stage E10.5, *Ripk1*$^{-/-}$ mice on a mixed 129/Sv C57BL/6 background die within 3 days of birth (Kelliher et al., 1998). However, survival of the *Ripk1*$^{-/-}$ mice was prolonged to 12 days after birth by *Tnfr1* deletion (Cusson et al., 2002).

Although *Tnfr1* deletion provides protection from *Ripk1*$^{-/-}$ perinatal lethality, it is incomplete, and the reason for the death of *Ripk1*$^{-/-}$ mice remains enigmatic. We therefore sought to determine the cause of this lethality. We show that, on a C57BL/6 background, *Ripk1*$^{-/-}$ mice die at birth from systemic inflammation, but they can be partially protected by deleting *Myd88* and thereby blocking IL-1 family and TLR inflammatory signaling. Furthermore, the embryonic lethality of *Casp8*$^{-/-}$ mice can be prevented by loss of RIPK1; however, loss of caspase-8 cannot protect *Ripk1*$^{-/-}$ mice from systemic inflammation and perinatal death. On the other hand, loss of the essential effectors of necroptosis, RIPK3 or MLKL, provides protection to *Ripk1*$^{-/-}$ mice from systemic inflammation but fails to correct a lethal intestinal defect. *Ripk1* deficiency-induced inflammation was associated with the release of IL-33, suggesting that this cytokine is a necroptotic danger-associated molecular pattern (DAMP) in vivo. Finally, we show that *Ripk1*$^{-/-}$*Ripk3*$^{-/-}$*Casp8*$^{-/-}$ mice were protected from inflammation and intestinal disruption and are viable and fertile. These results add to our understanding of the role of RIPK1 in regulating cell-death-inflammatory signaling pathways and demonstrate that necroptotic cell death can initiate a lethal inflammatory cascade.

RESULTS

RIPK1 Deficiency Results in Perinatal Lethality Marked by Systemic Cell Death

Ripk1$^{-/-}$ mice die within 3 days of birth on a mixed 129/Sv C57BL/6 background (Kelliher et al., 1998). After more than ten crosses with C57BL/6 mice, we found that *Ripk1*$^{-/-}$ mice develop severe multiorgan inflammation in utero and die within minutes of birth or Caesarean section. *Ripk1*$^{-/-}$ neonates appeared edematous and cyanotic (Figure 1A). The rapid cyanosis of *Ripk1*$^{-/-}$ neonates and labored breathing (Figure 1B) suggests that respiratory failure is the major cause of perinatal lethality. Cell death was the most striking histopathological finding with large necrotic regions in the liver and thymus (Figure 1C and Figure S1 and Table S2 available online) and cleaved caspase-3 (CC3)-positive cells in lung, liver, intestine, and thymus (Figures 1D and S1). CC3 and -8 were also detectable in plasma from *Ripk1*$^{-/-}$, but not *Ripk1*$^{+/+}$ neonates (Figure 1E). *Ripk1*$^{-/-}$ neonates had epidermal hyperplasia with no signs of CC3 (Figures 1C and 1D). Keratin-6 expression, which is normally confined to hair follicles in healthy skin, was also aberrantly expressed in *Ripk1*$^{-/-}$ epidermis (Figure 1C).

Ripk1$^{-/-}$ Neonates Exhibit Systemic Inflammation

Inflammatory cytokines were upregulated in the skin (Figure 2A), plasma (Figure 2B), liver, lung, and intestine (Figure S2A). *Ripk1*$^{-/-}$ neonates also had severe anemia and neutrophilia (Figures 2C–2E, S2B, and S2C), which is consistent with the elevated levels of proinflammatory cytokines and chemokines in the plasma; granulocyte colony-stimulating factor (G-CSF) was elevated >10^5-fold (Figures 2B and S2A). Surprisingly, given these results, the number of leukocytes in various tissues was reduced (Figures 2F and S1).

RIPK1 Is Required for Normal Hematopoiesis

To assess whether the inflammatory *Ripk1*$^{-/-}$ phenotype was transferable, we transplanted lethally irradiated mice with wild-type (WT) or *Ripk1*$^{-/-}$ fetal liver cells taken at embryonic day (E) 13.5. There was no evidence of inflammatory disease in recipient mice (Figure S3A); however, *Ripk1*$^{-/-}$ hematopoietic cells failed to engraft efficiently, with deficits in both myeloid and lymphoid lineages evident 8 weeks posttransplant (Figures 3A and 3B). Furthermore, at 14 and 26 weeks, an almost-complete loss of myeloid and lymphoid donor *Ripk1*$^{-/-}$ cells was observed (Figure 3A). Embryonic WT progenitor cells express RIPK1 (Figure S3B), and *Ripk1*$^{-/-}$ embryos had a normal hematopoietic progenitor cell compartment at E13.5 but a decrease in granulocyte-macrophage progenitors and megakaryocyte-erythroid progenitors at P0 (Figure 3C). Furthermore, the functional potential of *Ripk1*$^{-/-}$ embryonic progenitors remained normal ex vivo (Figure 3D). This suggests that the deficits observed in *Ripk1*$^{-/-}$ hematopoietic progenitor cells at P0 are a reflection of the systemic inflammation in these mice, but this does not account for the deficit when fetal liver cells are used to reconstitute mice (Figure 3C). Competitive transplantation of *Ripk1*$^{-/-}$ and WT fetal liver cells at a 1:1 ratio into lethally irradiated recipient mice revealed that WT cells outcompeted *Ripk1*$^{-/-}$ cells (Figure 3E), suggesting a cell-intrinsic defect in *Ripk1*$^{-/-}$ hematopoietic stem and progenitor cells (HSPC). Furthermore, lethally irradiated recipient mice receiving a serial transplant of either 0.2×10^6 or 1×10^6 *Ripk1*$^{-/-}$ bone marrow (BM) cells failed to thrive and succumbed to BM failure within 3 weeks (Figure 3F). These results demonstrate that *Ripk1*$^{-/-}$ HSPC are defective in their ability to self-renew. Mice transplanted with 5×10^6 *Ripk1*$^{-/-}$ BM cells survived similarly to mice receiving 0.2×10^6 WT cells, indicating that an increase in *Ripk1*$^{-/-}$ donor cells can partially compensate for this cell-intrinsic defect (Figure 3G).

TNF Neutralization Rescues the *Ripk1*$^{-/-}$ Emergency Hematopoiesis Defect

Because RIPK1 regulates TNF signaling and TNFR1 is upregulated in donor and recipient-derived hematopoietic cells in the bone marrow following transplantation (Pearl-Yafe et al., 2010;

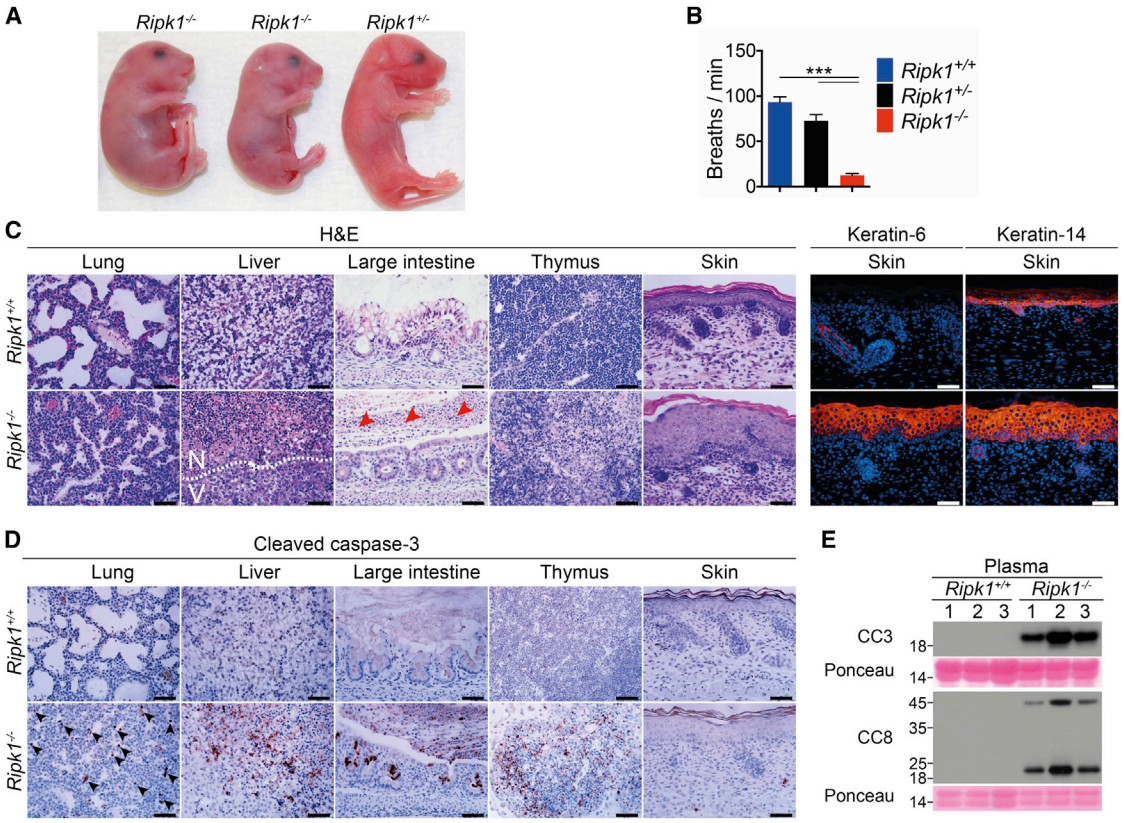

Figure 1. *Ripk1*$^{-/-}$ Neonates Die at Birth and Exhibit Multiorgan Pathology

(A) Neonates of indicated genotypes.

(B) Respiratory rates of neonates taken within minutes of Caesarean, n $\geq$ 3, columns show mean + SEM, ***p $\leq$ 0.005.

(C) Tissue sections of *Ripk1*$^{+/+}$ and *Ripk1*$^{-/-}$ mice stained with H&E, anti-keratin-6, or anti-keratin-14 (Red). Nuclei in immunofluorescence sections were counterstained with Hoechst (blue). N, necrotic and V, viable regions of liver. Red arrows, luminal slough. Each image is representative of at least three mice.

(D) Tissue sections stained with anti-CC3 (brown) and hematoxylin (blue). Black arrows, cleaved-caspase-3-positive cells. Each image is representative of at least three mice.

(E) Western blot of plasma from P0 mice of each genotype, n = 3, probed for cleaved caspase-3 (CC3) and cleaved caspase-8 (CC8), Ponceau S loading control. All data were obtained from neonates delivered by Caesarean at P0. All scale bars, 50 μm.

Weill et al., 1996), we hypothesized that deregulated TNF-TNFR1 signaling may cause the *Ripk1*$^{-/-}$ engraftment defect. We therefore investigated whether TNF or other death ligands mediated this defect. Indeed, *Ripk1*$^{-/-}$ progenitors were more sensitive to TNF and FasL as determined by their short-term survival (Figure S3C). Similarly, the yield of macrophages derived from *Ripk1*$^{-/-}$ fetal liver was reduced (Figure S3D), and they were sensitive to TNF-induced cell death (Figure S3E). Finally, we repeated the engraftment experiments with a TNF blocking antibody that rescued the reconstitution defect (Figure 3H). These reconstituted mice did not show signs of inflammation. Together, these results suggest that loss of RIPK1 sensitizes hematopoietic cells, including progenitors, to TNF-induced cell death, but this intrinsic defect, in isolation, is insufficient to initiate inflammatory disease.

Loss of TNFR1, FasL, or Caspase-8 Does Not Prevent *Ripk1*$^{-/-}$ Lethality

To examine the contribution of apoptotic signaling to *Ripk1*$^{-/-}$ neonatal lethality, we generated *Ripk1*$^{-/-}$*Tnfr1*$^{-/-}$ mice. In contrast to the partial suppression previously observed with *Tnfr1* deletion on the mixed 129/Sv background (Cusson et al., 2002), loss of *Tnfr1* did not provide meaningful protection on the C57BL/6 background, and *Ripk1*$^{-/-}$*Tnfr1*$^{-/-}$ neonates died within half an hour of birth (Figure 4A). Combined deficiency of TNF and the cell death ligand, FasL, also failed to prevent the *Ripk1*$^{-/-}$ lethality (Figures 4A and 4B).

To test the direct contribution of the extrinsic apoptotic pathway to the *Ripk1*$^{-/-}$ phenotype, we generated *Ripk1*$^{-/-}$*Casp8*$^{-/-}$ mice. Despite the fact that loss of caspase-8 results in lethality at E10.5 (Varfolomeev et al., 1998), these mice survived to birth. However, *Ripk1*$^{-/-}$*Casp8*$^{-/-}$ neonates were indistinguishable from their littermate *Ripk1*$^{-/-}$ controls and died minutes after birth (Figure 4A). *Ripk1*$^{-/-}$*Casp8*$^{-/-}$ and *Ripk1*$^{-/-}$*Tnfr1*$^{-/-}$ mice had the elevated white blood cell count, anemia, and inflammation seen in *Ripk1*$^{-/-}$ neonates (Figures 4B, 4C, S4A, and S4B). Likewise, *Ripk1*$^{-/-}$*Casp8*$^{-/-}$ and *Ripk1*$^{-/-}$*Tnfr1*$^{-/-}$ mice still had CC3 present in the plasma, as well as epidermal hyperplasia and aberrant keratin-6 expression (Figures 4D, 4E, and S4C). On the other hand, the large intestinal phenotype in *Ripk1*$^{-/-}$ mice was partially and completely

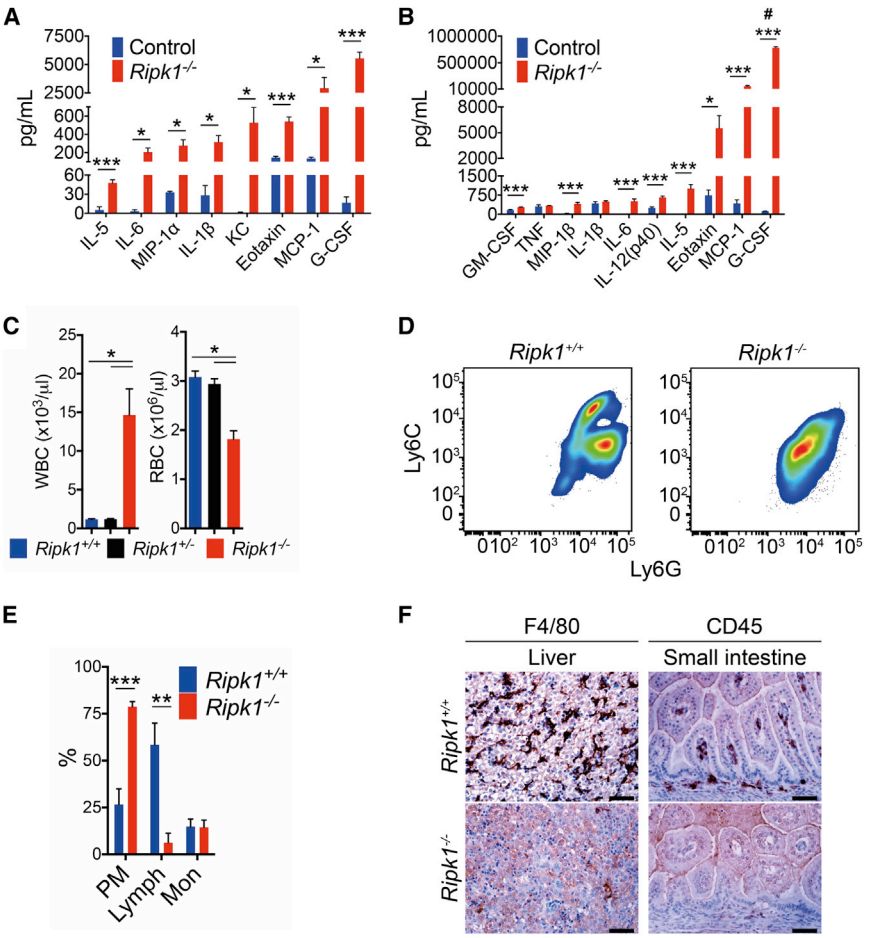

Figure 2. RIPK1 Is Required to Inhibit Systemic Inflammation, Anemia, and Neutrophilia

(A and B) Skin, n = 3 (A) and plasma, n = 5 (B) cytokine levels assayed using Bioplex. Number symbol (#), four of five values for plasma G-CSF were above the reference range and assigned value of highest standard. Controls, *Ripk1*$^{+/+}$ or *Ripk1*$^{+/-}$.

(C) Blood cells quantified with an ADVIA, n ≥ 4. WBC, white blood cells; RBC, red blood cells.

(D) Flow cytometric analysis of CD11b^{+} peripheral blood cells, Ly6G^{+}ly6C^{int}, neutrophils; Ly6C^{hi}, inflammatory monocytes; Ly6C^{low}, resident monocytes.

(E) Differential counts obtained from blood smears, n ≥ 4. PM, polymorphs; Lymph, lymphocytes; Mon, monocytes.

(F) Tissue sections stained with anti-F4/80 or anti-CD45. Each image is representative of at least three mice. Data were obtained from neonates delivered by Caesarean at E20.5 (A) or E19.5 (B–F). All graphs show mean values + SEM, *p ≤ 0.05, **p ≤ 0.01, and ***p ≤ 0.005. All scale bars, 50 μm.

suppressed in *Ripk1*$^{-/-}$*Tnfr1*$^{-/-}$ and the *Ripk1*$^{-/-}$*Casp8*$^{-/-}$ neonates, respectively, and correlated with the lack of CC3 in the intestine (Figures 4F and S4C).

RIPK3 and MLKL Deficiency Prevents *Ripk1*$^{-/-}$ Systemic Inflammation

According to prevailing models, loss of RIPK1 should block necroptosis. However, the fact that loss of *Casp8*, and therefore apoptosis, did not protect *Ripk1*$^{-/-}$ mice from perinatal lethality caused us to re-examine this. We therefore hypothesized that excessive necroptotic cell death occurs in *Ripk1*$^{-/-}$ neonates and generated *Ripk1*$^{-/-}$*Ripk3*$^{-/-}$ and *Ripk1*$^{-/-}$*Mlkl*$^{-/-}$ mice to test this. Remarkably, these mice appeared normal at birth (Figure 5A). Cell death that was visible by hematoxylin and eosin staining (H&E) was also reduced in these mice, and CC3 was undetectable in their plasma and reduced in all organs except the intestine (Figures 5B, 5C, and S5F). Consistent with necroptotic cell death driving inflammation, *Ripk1*$^{-/-}$*Ripk3*$^{-/-}$ and *Ripk1*$^{-/-}$*Mlkl*$^{-/-}$ mice mostly had normal keratin-6 and -14 expression (Figures 5D and S5G and Table S3) and normal white and red blood cell levels at P0 and P3 (Figures 5E and S5B), and leukocyte levels in tissues were restored (Figure S5F). These mice also had reduced inflammatory cytokine levels at these time points (Figures 5F and S5D) compared to the *Ripk1*$^{-/-}$ mice. Nevertheless, *Ripk1*$^{-/-}$*Ripk3*$^{-/-}$ and *Ripk1*$^{-/-}$*Mlkl*$^{-/-}$ mice failed to thrive, had hypoglycemia (Figures 5A, 5G, and S5A) despite being fed, and did not survive past postnatal day 4 (P4). Compound *Ripk3* deficiency also partially suppressed the defect of *Ripk1*$^{-/-}$ hematopoietic cells at 8 weeks posttransplant in primary and serial transplant recipient mice (Figures 5H and S5E).

We sought to correlate these changes with molecular markers of apoptosis and necroptosis. Remarkably, RIPK3, MLKL, and cFLIP levels were all elevated in *Ripk1*$^{-/-}$ skin when compared to WT controls (Figures 5I and 5J). This elevated cFLIP could inhibit caspase-8-induced apoptosis and, together, with the elevated levels of the necroptotic effectors, provides a potential explanation for the suppression of *Ripk1*$^{-/-}$ keratinocyte hyperplasia by combined loss of MLKL or RIPK3.

Ripk1$^{-/-}$ Systemic Inflammation Is Not Driven by the Inflammasome

Because pyroptosis, a caspase-1-dependent cell death, can result in systemic inflammation and was suggested to be dependent on RIPK3 in BMDM and BMDC models, we tested the possibility that the inflammasome is activated in *Ripk1*$^{-/-}$ mice. Lipopolysaccharide (LPS) priming in *Ripk1*$^{-/-}$ fetal liver-derived macrophages (FLDM), without an inflammasome stimulus, resulted in secretion of low levels of cleaved IL-1β and caspase-1 (Figures 6A and S6A). In agreement with earlier reports (Kang et al., 2013; Vince et al., 2012), this active inflammasome status in *Ripk1*$^{-/-}$ FLDM was RIPK3 dependent (Figures 6A and S6A). In vitro, this indicates that *Ripk1*$^{-/-}$ macrophages have constitutive low-level inflammasome activity. In vivo, however, we could not detect signs of inflammasome activation—on

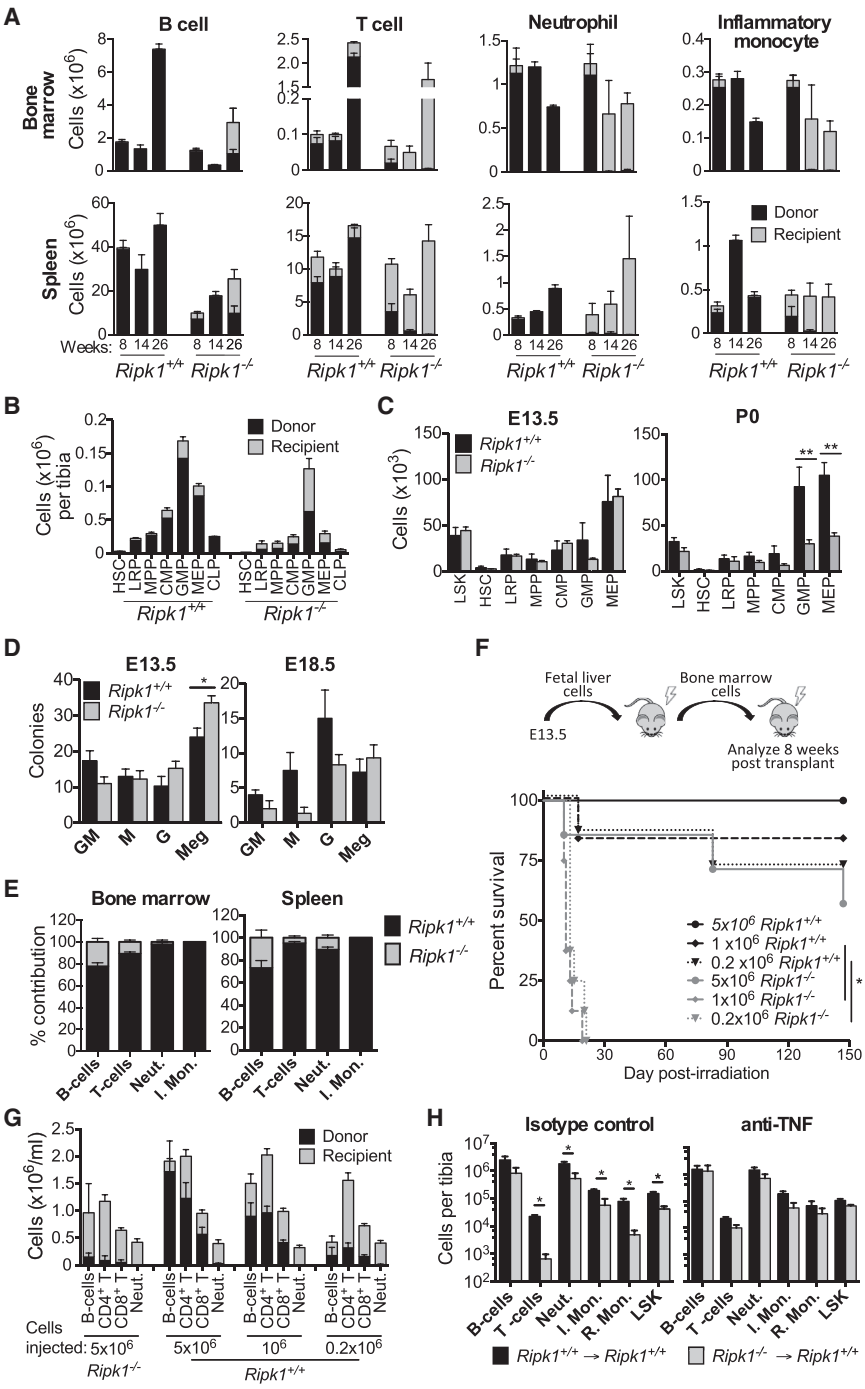

Figure 3. RIPK1 Is Required for Normal Hematopoiesis

(A) Contribution of donor and recipient cells in the bone marrow and spleen of lethally irradiated recipients 8, 14, and 26 weeks posttransplant, n = 3–7.

(B) Counts of hematopoietic stem cells (HSC), lineage-restricted progenitors (LRP), multipotent progenitors (MPP), common myeloid progenitors (CMP), granulocyte-macrophage progenitors (GMP), megakaryocyte-erythroid progenitors (MEP), and common lymphoid progenitors (CLP) from the bone marrow of lethally irradiated recipients 8 weeks posttransplant, n = 3–7.

(C) Counts of *Ripk1*$^{+/+}$ and *Ripk1*$^{-/-}$ liver progenitors at E13.5 and P0, n $\geq$ 4.

(D) Differentiation of E13.5 and E18.5 fetal liver progenitors after 7 days of culture in SCF+IL-3+EPO. Granulocyte (G), macrophage (M), granulocyte-macrophage (GM), and megakaryocyte (Meg) colonies, n = 3–7.

(E) Contribution of *Ripk1*$^{+/+}$ and *Ripk1*$^{-/-}$ cells in bone marrow and spleen of lethally irradiated recipients transplanted with equal numbers of *Ripk1*$^{+/+}$ and *Ripk1*$^{-/-}$ fetal liver cells 8 weeks posttransplant, n = 5.

(F) Survival of serial transplant recipients, transplanted with 0.2 × 10^6–5 × 10^6 bone marrow cells from *Ripk1*$^{+/+}$ or *Ripk1*$^{-/-}$ reconstituted mice, n = 5–8.

(G) Contribution of donor and recipient blood cells in serial transplant recipients from (F) 8 weeks posttransplant.

(H) Analysis of bone marrow from reconstituted mice at 8 weeks. Where indicated, recipient mice were treated with TNF-blocking antibody or isotype control (Iso) three times per week for 2 weeks then weekly for 6 weeks, n = 6 mice per group. Neut, neutrophil; I. Mon, inflammatory monocyte; R. Mon, resident monocyte; LSK, Lin$^-$Sca-1$^+$c-Kit$^+$. All graphs show mean + SEM; *p $\leq$ 0.05 and **p $\leq$ 0.01.

the contrary, caspase-1 and IL-1β were present in the pro, uncleaved form in tissue and plasma (Figures 6B–6D). Thus, we conclude that the inflammasome plays little to no role in *Ripk1*$^{-/-}$ neonatal systemic inflammation.

The Necroptotic DAMPs, IL-1α and IL-33, Correlate with *Ripk1*$^{-/-}$ Inflammation

Several DAMPs, including HMGB1, IL-1α, and IL-33, have been suggested to be released from necroptotic cells. The relative importance of these DAMPs in vivo is unknown (Kaczmarek et al., 2013). HMGB1 levels in the plasma of *Ripk1*$^{-/-}$ and WT neonates were identical (Figure 6E). On the other hand, there were high levels of IL-1α and IL-33 in the plasma of *Ripk1*$^{-/-}$ neonates (Figures 6F and 6G). Furthermore, IL-33 expression was elevated in the skin and intestine of *Ripk1*$^{-/-}$ neonates and was released as a processed and inflammatory form (Lefrançais et al., 2012) in the plasma of *Ripk1*$^{-/-}$ and *Ripk1*$^{-/-}$*Casp8*$^{-/-}$ mice, but not in *Ripk1*$^{-/-}$*Mlkl*$^{-/-}$ or *Ripk1*$^{-/-}$*Ripk3*$^{-/-}$ mice, indicating an important role for necroptotic death in IL-33 production (Figure 6G).

MyD88 Deficiency Suppresses *Ripk1*$^{-/-}$ Inflammation

MyD88 is an essential component of IL-1, IL-33, and a subset of TLR signaling complexes (Beutler et al., 2006). We therefore

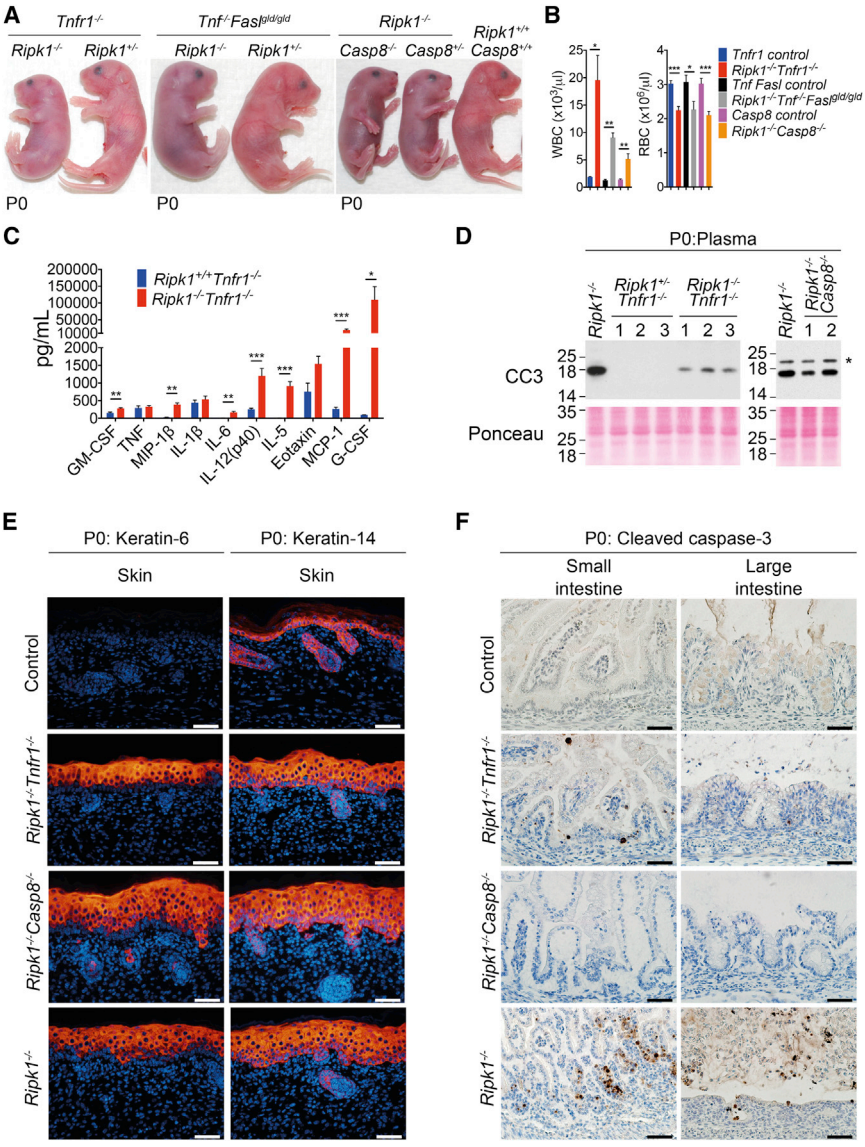

Figure 4. *Tnfr1* and *Casp8* Deficiency Provides No Survival Advantage to *Ripk1*$^{-/-}$ Neonates but Ameliorates the Large Intestine Phenotype

(A) Neonates of indicated genotype obtained after Caesarean delivery at P0.

(B) Blood cell quantification using an ADVIA, n ≥ 3. WBC, white blood cells; RBC, red blood cells. *Tnfr1* control, *Ripk1*$^{+/+}$*Tnfr1*$^{-/-}$. *TnfFasl* control, *Ripk1*$^{+/-}$ *Tnf*$^{-/-}$*Fasl*$^{gld/gld}$. *Casp8* control, *Ripk1*$^{+/+ \text{ or } +/-}$ *Casp8*$^{+/+ \text{ or } +/-}$.

(C) Plasma cytokine levels of P0 mice assayed using Bioplex, n = 4.

(D) Western blot of plasma from three *Ripk1*$^{-/-}$ *Tnfr1*$^{-/-}$ and two *Ripk1*$^{-/-}$*Casp8*$^{-/-}$ mice probed for cleaved caspase-3 (CC3). Ponceau S loading control. Asterisk (*) indicates nonspecific band.

(E) Immunofluorescence analysis of skin sections stained with anti-keratin-6, anti-keratin-14 (red), or Hoechst nuclear stain (blue).

(F) Tissue sections stained with anti-CC3 (brown) and hematoxylin (blue).

(E and F) Each image is representative of at least three mice. Control, WT.

All graphs are mean + SEM. *p ≤ 0.05, **p ≤ 0.01, and ***p ≤ 0.005.

Caspase-8 Deficiency Prevents *Ripk1*$^{-/-}$*Ripk3*$^{-/-}$ Lethality

The areas of enterocyte cell death and CC3-positive cells in *Ripk1*$^{-/-}$*Ripk3*$^{-/-}$, *Ripk1*$^{-/-}$*Mlkl*$^{-/-}$, and *Ripk1*$^{-/-}$*Myd88*$^{-/-}$ mice, which progressively worsen from birth to P3, raised the possibility that defective gastrointestinal function may be the underlying cause of death in these compound knockout mice. One obvious possibility was that bacterial colonization after birth leads to TNF production and intestinal cell death; however, *Ripk1*$^{-/-}$*Ripk3*$^{-/-}$ mice generated in an abiotic environment were not protected from early death (Table S1).

hypothesized that *Myd88* deficiency could provide a survival advantage to *Ripk1*$^{-/-}$ mice by reducing these inflammatory pathways. In contrast to the lack of suppression of the *Ripk1*$^{-/-}$ phenotype observed with *Tnfr1* deletion, *Ripk1*$^{-/-}$*Myd88*$^{-/-}$ neonates appeared relatively normal at birth and had mild to no edema (Figure 6H). Unfortunately, like the *Ripk3*$^{-/-}$ and *Mlkl*$^{-/-}$ crosses, the mice failed to thrive and only survived about 4 days from birth (Figure S6B). Deletion of *Myd88* reduced neutrophilia, prevented the anemia, and dramatically reduced the inflammation seen in *Ripk1*$^{-/-}$ neonates (Figures 6I, 6J, S6C, and S6D). At P0, epidermal hyperplasia and CC3 in the plasma were still observed in *Ripk1*$^{-/-}$*Myd88*$^{-/-}$ neonates (Figures 6K and S6F and Table S1). Nevertheless, in surviving mice (P3), *Myd88* loss prevented the epidermal hyperplasia, but not the intestinal CC3 and the low blood glucose seen in *Ripk1*$^{-/-}$ neonates (Figures 6L, 6M, S6E, and S6F).

To test whether the loss of gastrointestinal function was the result of excessive caspase-8-dependent apoptosis in the *Ripk1*$^{-/-}$*Ripk3*$^{-/-}$ and *Ripk1*$^{-/-}$*Mlkl*$^{-/-}$ mice, as suggested by the prevention of the intestinal pathology in the *Ripk1*$^{-/-}$*Casp8*$^{-/-}$ mice, we generated *Ripk1*$^{-/-}$*Ripk3*$^{-/-}$*Casp8*$^{-/-}$ mice. These mice were viable and fertile and put on weight like their WT counterparts (Figures 7A and S7A). CC3 was absent from the intestine and plasma, and the mice displayed none of the *Ripk1*$^{-/-}$ inflammatory pathology (Figures 7B, 7C, S7B, S7C, and S7F–S7I and Table S3). Furthermore, unlike *Ripk1*$^{-/-}$ fetal liver cells, *Ripk1*$^{-/-}$*Ripk3*$^{-/-}$*Casp8*$^{-/-}$ cells were not outcompeted by WT cells in a competitive transplant assay (Figures 7D and S7J). When aged, these mice developed the lymphoproliferative syndrome (Figures 7E–7G, S7D, and S7E) seen in *Casp8*$^{-/-}$*Ripk3*$^{-/-}$ mice (Kaiser et al., 2011; Oberst et al., 2011). However, the severity of this disease was attenuated in

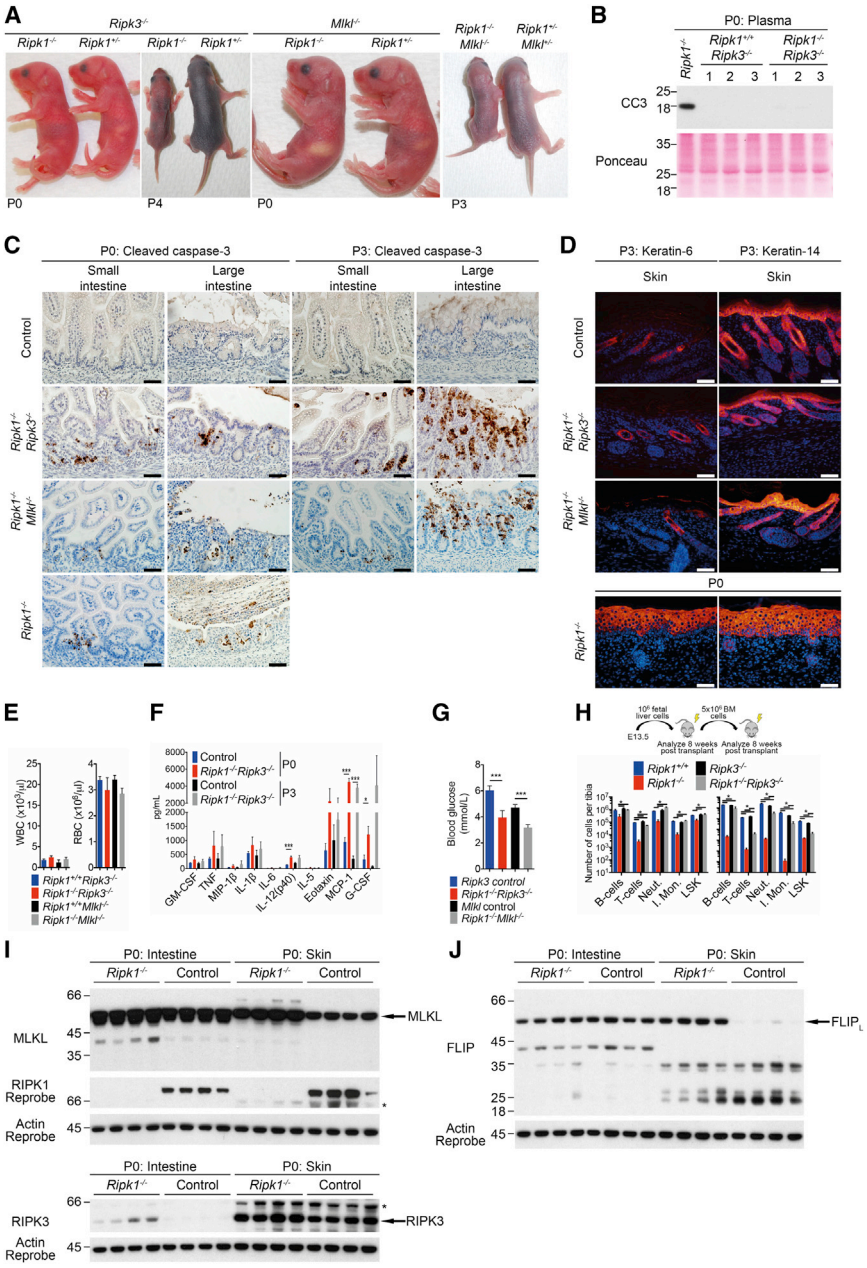

Figure 5. *Ripk1*$^{-/-}$ Lethality Is Partly Mediated by RIPK3 and MLKL

(A) *Ripk1*$^{-/-}$*Ripk3*$^{-/-}$ and *Ripk1*$^{-/-}$*Mlkl*$^{-/-}$ mice and littermate controls at P0, P3, or P4.

(B) Western blot of plasma from three P0 mice of each genotype probed for CC3. Ponceau S loading control.

(C) Tissue sections of P0 or P3 mice stained with anti-CC3 (brown) and hematoxylin (blue).

(D) Skin sections from indicated genotype stained with anti-keratin-6 or anti-keratin-14 (red) counterstained with Hoechst (blue). *Ripk1*$^{-/-}$ images in (D) are duplicated from Figure 1 for purposes of reference.

(C and D) Each image is representative of at least three mice. Control, *Ripk1*$^{+/+\ or\ +/-}$*Ripk3*$^{-/-}$.

(E) Blood cells from P0 mice quantified using ADVIA, n ≥ 3. WBC, white blood cells; RBC, red blood cells.

(F) Plasma cytokine levels of P0 or P3 mice assayed using Bioplex, n ≥ 3. Control, *Ripk1*$^{+/+\ or\ +/-}$*Ripk3*$^{-/-}$.

(G) Blood glucose levels from P3 mice quantified using an Accu-Chek glucometer; *Ripk3* control, *Ripk1*$^{+/+\ or\ +/-}$ *Ripk3*$^{-/-}$, n = 32; *Ripk1*$^{-/-}$*Ripk3*$^{-/-}$, n = 11; *Mlkl* control; *Ripk1*$^{+/+\ or\ +/-}$ *Mlkl* $^{+/-\ or\ -/-}$, n = 8; *Ripk1*$^{-/-}$*Mlkl*$^{-/-}$, n = 4.

(H) Blood cell counts from bone marrow of WT recipient mice transplanted with 1 × 10^6 fetal liver cells of the indicated genotypes and then serially transplanted with 5 × 10^6 BM cells. Analysis was performed 8 weeks posttransplant using flow cytometry. Neut, neutrophil; I. Mon, inflammatory monocyte; LSK, Lin$^-$Sca-1$^+$c-Kit$^+$.

(I and J) Western blot of tissue lysates probed with the indicated antibodies. *Ripk1*$^{-/-}$, n = 4; *Ripk1*$^{+/+\ or\ +/-}$, n = 4. The asterisk (*) indicates a nonspecific band.

All graphs depict mean + SEM. *p ≤ 0.05 and ***p ≤ 0.005.

a *Ripk1* dose-dependent manner, such that splenomegaly was almost abolished in the *Ripk1*$^{-/-}$*Ripk3*$^{-/-}$*Casp8*$^{-/-}$ mice and reduced in the *Ripk1* heterozygotes at 16–18 weeks (Figures 7E and 7F). Likewise, infiltration of CD3$^+$B220$^+$ cells into peripheral organs was reduced by loss of *Ripk1* (Figure 7G).

DISCUSSION

We show that C57BL/6 *Ripk1*$^{-/-}$ neonates succumb to a cell-death-induced inflammatory phenotype with multiorgan pathology (Table S1). *Ripk1*$^{-/-}$ mice on a mixed 129/Sv C57BL/6 background died within 3 days of birth (P3) (Kelliher et al., 1998), but by the fourth backcross of mixed background *Ripk1*$^{-/-}$ to C57BL/6 mice, we were unable to recover viable knockout mice at P0. The 129/Sv strain is mutant for caspase-11, and some of the phenotype previously ascribed to loss of caspase-1, a closely linked gene in the same 9qA1 chromosomal location, is due to the loss of caspase-11 (Kayagaki et al., 2011). However, RIPK1 is on murine chromosome 13, and therefore, given the extent of the backcross needed to reveal the perinatal lethality, functional caspase-11 is unlikely to be the modifier. The importance of the genetic background is emphasized by the role of *Tnfr1* in the *Ripk1*$^{-/-}$ phenotype. C57BL/6 129/Sv *Ripk1*$^{-/-}$*Tnfr1*$^{-/-}$ mice survive up to 12 days after birth (Cusson et al., 2002). Remarkably, however, given the focus on the role of RIPK1 in TNF signaling, *Ripk1*$^{-/-}$ lethality at birth was not prevented at all by deletion of *Tnfr1* on a C57BL/6 background, although the disrupted intestinal phenotype was.

Cusson et al. (2002) reported that *Ripk1*$^{-/-}$ thymocytes were reduced 6 weeks after transplant of *Ripk1*$^{-/-}$ fetal liver cells

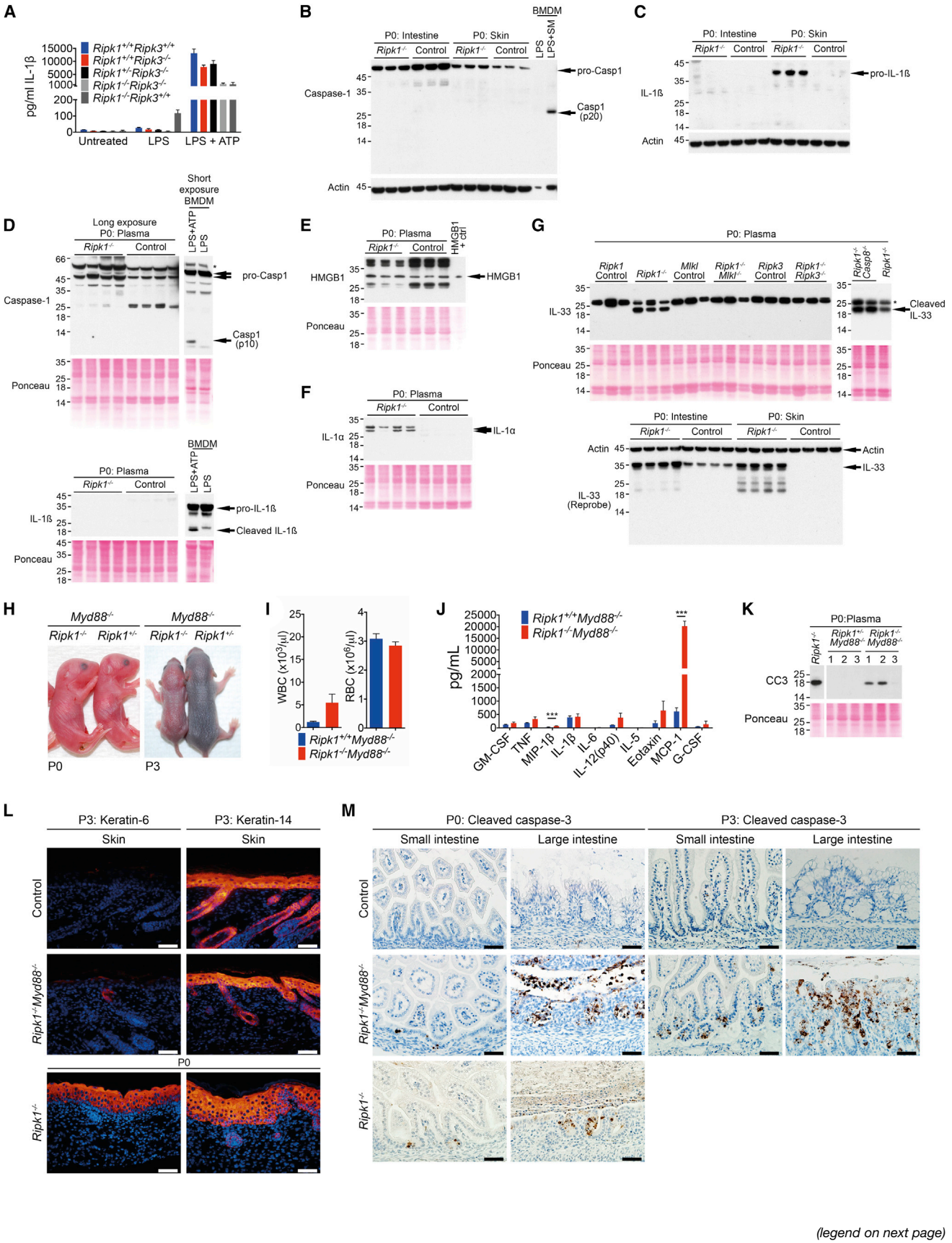

(legend on next page)

into lethally irradiated mice and died in a TNFR2-dependent manner, but B and myeloid cell numbers appeared normal. We found that B- and T-lymphoid and neutrophil numbers were reduced 8 weeks posttransplant in the absence of RIPK1. Furthermore, at this time, there were deficits in progenitor cell numbers, and, by 14 weeks, profound defects in the ability of *Ripk1*$^{-/-}$ cells to reconstitute all hematopoietic compartments became apparent. During engraftment, a model of emergency hematopoiesis, hematopoietic stem cells must rapidly generate large numbers of mature cells for the recipient to survive. Our results demonstrate that TNF, which was shown to be upregulated during emergency hematopoiesis (Weill et al., 1996), plays a role in the *Ripk1*$^{-/-}$ engraftment defect because administration of neutralizing TNF antibodies suppressed the emergency hematopoietic defect. Similarly, loss of caspase-8 also causes B, T, and progenitor cell defects in *Rag1*$^{-/-}$ reconstituted mice (Kang et al., 2004). Together, with our result that compound deficiency of *Ripk3* partially prevented the reconstitution defects seen in *Ripk1*$^{-/-}$ hematopoietic cells, this suggests that both apoptotic and necroptotic pathways are activated by TNF in *Ripk1*$^{-/-}$ hematopoietic cells during engraftment. Consistent with this, we observed that *Ripk1*$^{-/-}$*Ripk3*$^{-/-}$*Casp8*$^{-/-}$ fetal liver cells were able to compete with WT cells in a competitive transplant. These results demonstrate that there are TNF-dependent roles for RIPK1 in stress-induced hematopoiesis and that TNF appears to license hematopoietic stem and progenitor cells entering the bone marrow during inflammation by delivering a RIPK1-dependent survival signal. These experiments also showed that *Ripk1*$^{-/-}$ cells do not transfer the inflammatory phenotype into WT recipients. One caveat to this conclusion is that *Ripk1*$^{-/-}$ fetal liver cells do not reconstitute properly. However, at 8 weeks posttransplant, there appear to be sufficient numbers of *Ripk1*$^{-/-}$ neutrophils and monocytes to drive inflammatory disease. Furthermore, *Ripk1*$^{-/-}$ reconstitutions treated with anti-TNF successfully engrafted but failed to transfer the inflammatory phenotype. Because TNF plays little to no role in the systemic inflammation in *Ripk1*$^{-/-}$ mice, it seems unlikely that the hematopoietic compartment, in isolation, is a major initiator of the inflammatory phenotype.

Despite the fact that TNF/TNFR1 signaling does not play a significant role in *Ripk1*$^{-/-}$ lethality, RIPK1 clearly has a protective role in TNF signaling. In this role, it provides a platform for recruitment of kinases that are required to activate NF-κB and thereby upregulate antiapoptotic proteins, principally cFLIP, to prevent activation of caspase-8 and -3 and apoptosis (Schmukle and Walczak, 2012; Wertz and Dixit, 2010). The power of genetic experiments is that they test such models in global terms. Loss of RIPK1 in the mouse leads to massive cell death, associated with CC3 and -8; therefore, RIPK1 clearly plays a protective role during embryogenesis. However, there are important exceptions; for example, a TNF-dependent checkpoint exists at embryonic stage E10.5 (Dillon et al., 2014 [this issue of *Cell*]), and in the absence of cFLIP, mice die at this stage (Yeh et al., 2000). Because loss of RIPK1 does not lead to embryonic death at E10.5, then RIPK1 is not required to protect against TNF-driven lethality at E10.5. Furthermore, we can conclude that production of cFLIP at E10.5 is independent of RIPK1. More surprisingly still, loss of RIPK1 results in dramatic upregulation of cFLIP levels in the skin, turning the accepted model on its head in this tissue.

In other tissues, the cFLIP/RIPK1 axis may play a more important role. Conditional deletion of *cFlip* in intestinal epithelial cells (Piao et al., 2012) led to uncontrolled apoptosis and perinatal lethality (P2), which was prevented by deletion of *Tnfr1*. Although *Tnfr1* deletion did not prevent early lethality of *Ripk1*$^{-/-}$ mice, we observed reduction in cell death and pathology in the large intestine. Thus, the TNF/TNFR1/RIPK1 signaling axis plays an important role in the intestine, but the source of TNF is unknown. TNF/TNFR1 knockout mice have defective Peyer's patch formation (Korner et al., 1997), thus there might be a local, developmentally regulated source of TNF. Alternatively, the intestine of P0 *Ripk1*$^{-/-}$ mice may be exquisitely sensitive to systemic TNF circulating in these mice. *Ripk1*$^{-/-}$*Myd88*$^{-/-}$, *Ripk1*$^{-/-}$*Ripk3*$^{-/-}$, and *Ripk1*$^{-/-}$*Mlkl*$^{-/-}$ mice survive beyond birth and become colonized by bacteria. Thus, in these mice, it is possible that host-microbial interactions generate TNF. However, *Ripk1*$^{-/-}$*Ripk3*$^{-/-}$ mice raised in an abiotic environment had no survival advantage, indicating that host-microbiome interaction is not a significant factor in the lethality at P4. Similarly to *Tnfr1* deletion, *Casp8* deletion reduced cell death and pathology in the large intestine of *Ripk1*$^{-/-}$ mice. In agreement with our interpretation that the excessive intestinal apoptosis kills

Figure 6. *Ripk1*$^{-/-}$ Inflammatory Phenotype Is *Myd88* Dependent and Is Marked by the Presence of Cleaved IL-33 in the Plasma

(A) IL-1β secretion from E13.5 FLDMs, primed with ultrapure LPS (20 ng/ml) for 6–8 hr ± 5 mM ATP for 60 min were analyzed by ELISA, n ≥ 4.

(B and C) Western blot of skin and intestine tissue lysates probed with anti-caspase-1 (B) and anti-IL-1β (C), *Ripk1*$^{-/-}$, n = 3; *Ripk1*$^{+/+\ or\ +/-}$, n = 3. Supernatant from BMDMs treated with LPS ± Smac mimetic (SM) were used as controls for caspase-1 cleavage (B).

(D–F) Western blot of plasma from P0 mice probed with caspase-1 and IL-1β (D), HMGB1 (E), and IL-1α (F) antibodies; *Ripk1*$^{-/-}$, n ≥ 3; *Ripk1*$^{+/+\ or\ +/-}$, n ≥ 3. Ponceau S loading control. Asterisk (*) indicates nonspecific band. Lysates from BMDMs treated as per (A) were used as controls for caspase-1 and IL-1β cleavage (D). HMGB1-positive control is lysate from BMDMs (E).

(G) Western blot of plasma (top) and tissue (bottom) from P0 neonates with anti-IL-33. Skin and intestine controls, *Ripk1*$^{+/+}$ or *Ripk1*$^{+/-}$ mice; plasma controls, *Mlkl*$^{-/-}$, *Ripk3*$^{-/-}$ or WT for *Ripk1*$^{-/-}$. Asterisk (*) indicates nonspecific band.

(H) Neonates of indicated genotype obtained after Caesarean at P0 or P3.

(I) Blood cell quantification using ADVIA, n ≥ 3. WBC, white blood cells; RBC, red blood cells.

(J) Plasma cytokine levels of P0 mice assayed using Bioplex, n ≥ 3.

(K) Western blot of plasma from P0 mice; n = 3 of each genotype probed for CC3. Run on same gel as Figure 4D.

(L) Skin sections stained with anti-keratin-6 or anti-keratin-14 (red) and Hoechst (blue).

(M) Tissue sections of P0 or P3 mice stained with anti-CC3 (brown) and hematoxylin (blue).

(L and M) Each image is representative of at least three mice. Control, *Myd88*$^{-/-}$.

All graphs show mean + SEM. ***p ≤ 0.005. All scale bars, 50 μm.

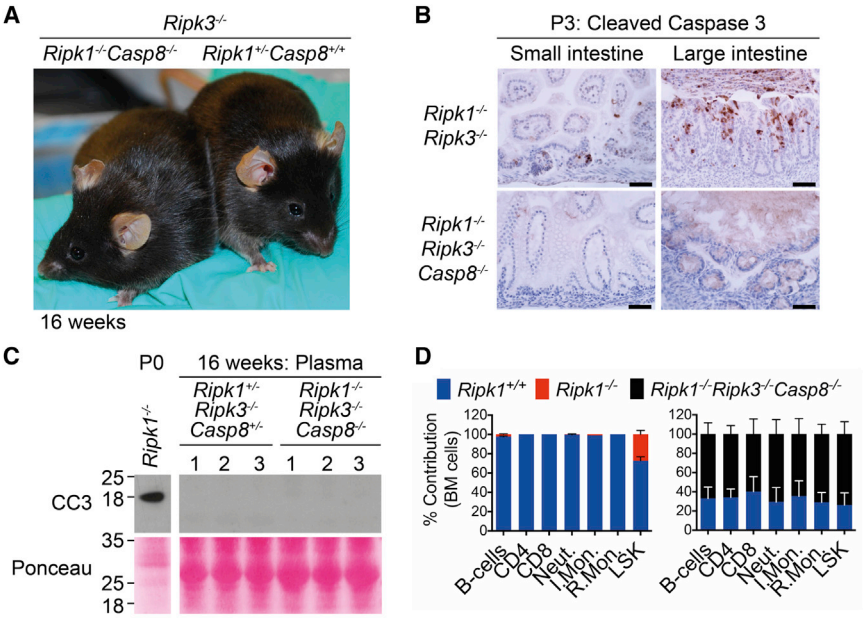

Figure 7. *Ripk1*$^{-/-}$*Ripk3*$^{-/-}$ Lethality Is Mediated by Caspase-8

(A) *Ripk1*$^{-/-}$*Ripk3*$^{-/-}$*Casp8*$^{-/-}$ and control *Ripk*$^{+/-}$ *Ripk3*$^{-/-}$*Casp8*$^{+/+}$ mice at 16 weeks.

(B) Tissue sections from P3 mice stained with anti-CC3. Each image is representative of three mice.

(C) Western blot of plasma from 17- to 18-week-old mice probed for CC3. Ponceau S loading control. Plasma from the P0 *Ripk1*$^{-/-}$ control was run on the same gel.

(D) Percentage contribution of recipient BM cells from lethally irradiated mice injected with a 1:1 ratio of fetal liver cells from indicated genotypes. Neut, neutrophil; I. Mon, inflammatory monocyte; LSK, Lin^{-}Sca-1^{+}c-Kit^{+}; n = 3 mice per group.

(E) Lymph nodes (LN), spleen, and thymus of 18-week-old mice of the indicated genotypes.

(F) Spleen weights of 16- to 18-week-old mice of the indicated genotypes.

(G) Percentage of CD3^{+}B220^{+} cells in the spleen, peripheral blood (PB), BM, and LN of 16- to 18-week-old mice.

All graphs show mean + SEM. *p $\leq$ 0.05. All scale bars, 50 μm.

Ripk1$^{-/-}$*Ripk3*$^{-/-}$ mice at P4, *Ripk1*$^{-/-}$*Ripk3*$^{-/-}$*Casp8*$^{-/-}$ mice survived to adulthood.

RIPK1 not only protects from TNF induced killing, but if caspase-8 activity is inhibited, then it is believed to be required for TNF- or TLR-induced necroptosis in a kinase-dependent manner. In part, this idea has arisen because the RIPK1 kinase inhibitor, necrostatin, blocks necroptosis, and therefore, RIPK1 kinase activity and necroptosis have become synonymous. A requirement for RIPK1 in necroptosis is suggested in the situation of the embryonic lethality of *Casp8*$^{-/-}$ mice at embryonic stage E10.5 because loss of *Ripk1*, like loss of *Ripk3*, prevents this lethality. However, the *Ripk1*$^{-/-}$ mouse shows that RIPK1 is not a universal requirement for necroptosis; if it were, then *Ripk1*$^{-/-}$*Casp8*$^{-/-}$ mice would be completely defective in both apoptotic and necroptotic pathways and phenocopy the viable *Ripk3*$^{-/-}$*Casp8*$^{-/-}$ mice. However, combined deletion of *Casp8* and *Ripk3* is required to protect *Ripk1*$^{-/-}$ mice, suggesting that RIPK3-dependent necroptotic cell death can be activated in a RIPK1-independent manner. The fact that the *Ripk1*$^{-/-}$*Mlkl*$^{-/-}$ mice phenocopy the *Ripk1*$^{-/-}$*Ripk3*$^{-/-}$ mice provides further support for the idea that there is physiological RIPK1-independent necroptosis. Such RIPK1-independent necroptosis is consistent with reports that oligomerization and activation of RIPK3 may be driven by spontaneously high RIPK3 levels or by another RHIM-containing protein such as DAI or TRIF (Feoktistova et al., 2011; Moujalled et al., 2013; Upton et al., 2010).

Counterintuitively keratinocyte hyperplasia is an excellent marker of excessive cell death in the skin as seen in the epidermal keratinocyte-specific knockouts (EKO): *cFlip*^{EKO}, *Ikbkb*^{EKO}, *Fadd*^{EKO}, *Casp8*^{EKO}, and Sharpin mutant mice (Bonnet et al., 2011; Gerlach et al., 2011; Panayotova-Dimitrova et al., 2013; Pasparakis et al., 2002). *Ripk1*$^{-/-}$ mice have a similar skin phenotype to these mice. Not only are MLKL and RIPK3 upregulated in the skin of *Ripk1*$^{-/-}$ mice, but cFLIP is as well. Combined upregulation of these necroptotic effectors and the caspase-8 inhibitor cFLIP strongly suggests that *Ripk1*$^{-/-}$ skin cells are dying a necroptotic cell death, and this conclusion is reinforced by the fact that the *Ripk1*$^{-/-}$ skin phenotype is largely prevented by loss of *Ripk3* or *Mlkl*, but not *Casp8*. Clearly, however, this necroptotic cell death is caused by loss of, and is not dependent upon, RIPK1.

Loss of RIPK3 prevents the early embryonic lethality observed in caspase-8 knockout mice (Kaiser et al., 2011; Oberst et al., 2011), suggesting that loss of caspase-8 results in unchecked RIPK3-dependent necroptosis. Although RIPK3 and caspase-8 are best known as cell death mediators, both have emerged as direct regulators of the inflammasome and other inflammatory signaling pathways (Kang et al., 2013; Vince et al., 2012). Therefore, an alternative explanation for the E10.5 lethality is that absence of caspase-8 leads to an increase in RIPK3-dependent inflammatory cytokine production and death. The late lethality of *Ripk1* knockout mice has facilitated delineation of the relative importance of these two functions because *Ripk1*$^{-/-}$*Ripk3*$^{-/-}$ mice have significantly less death and inflammation, whereas the *Ripk1*$^{-/-}$*Myd88*$^{-/-}$ mice have reduced inflammation but not dramatically reduced cell death. Further support for the idea that necroptosis can be a driver of lethal inflammation comes from the fact that *Ripk1*$^{-/-}$*Mlkl*$^{-/-}$ and *Ripk1*$^{-/-}$*Ripk3*$^{-/-}$ mice phenocopy each other with dramatically reduced inflammation. MLKL functions downstream of RIPK3 in the necroptotic pathway (Moujalled et al., 2013; Murphy et al., 2013; Sun et al., 2012; Zhao et al., 2012) and may be a direct necroptosis effector (Chen et al., 2014). Although MLKL may have a role in cytokine production mediated by the inflammasome in the absence of caspase-8 (Kang et al., 2013), it does not in response to Smac mimetics (Wong et al., 2014) or a TLR ligand (Figure S5C). Although *Ripk1*$^{-/-}$ FLDMs showed RIPK3-dependent spontaneous activation of the inflammasome, it was at very low levels compared to a conventional NLRP3 inflammasome stimulus such as ATP. Furthermore, the systemic inflammation in the *Ripk1*$^{-/-}$ mice was not associated with markers of inflammasome activation. Taken together, we believe our data favor the interpretation that necroptosis induces inflammation.

An outstanding question in the field is the nature of necroptotic DAMPs (Kaczmarek et al., 2013). Because the *Ripk1*$^{-/-}$ inflammatory phenotype is rampant before birth, in a sterile embryonic environment, the DAMPs must be endogenous in origin. We observed high numbers of apoptotic cells throughout the *Ripk1*$^{-/-}$ embryos, and contents from these uncleared cells could feasibly generate DAMPs. However, we do not favor this hypothesis because compound *Ripk1*$^{-/-}$*Casp8*$^{-/-}$ mice are not protected from inflammation. We favor the hypothesis that RIPK1-independent necroptotic cell death is the source of DAMPs because both *Ripk1*$^{-/-}$*Ripk3*$^{-/-}$ and *Ripk1*$^{-/-}$*Mlkl*$^{-/-}$ are protected from the lethal inflammatory disease. HMGB1 is released from necroptotic cells in vitro and has a role in certain in vivo inflammation models (Scaffidi et al., 2002), suggesting that it is a necroptotic DAMP. However, we did not observe release of HMGB1 into plasma above control levels. Two other DAMPs that have been associated with necroptosis, IL-1α and IL-33 (Kaczmarek et al., 2013), were detected in the plasma of *Ripk1*$^{-/-}$ mice. IL-33 was expressed at high levels in the intestine and skin of *Ripk1*$^{-/-}$. Furthermore, IL-33 was detected in a processed form that corresponded to a previously reported neutrophil cleaved bioactive form (Lefrançais et al., 2012). IL-1α is not released during apoptosis (Cohen et al., 2010), and IL-33 was suggested to be cleaved to a nonactive form (~p25 and ~p10) during apoptosis by caspase-3 (Lüthi et al., 2009). Combined with the fact that IL-33 release into the plasma of the *Ripk1*$^{-/-}$ neonates is prevented by the *Ripk3*$^{-/-}$ and *Mlkl*$^{-/-}$, but not the *Casp8*$^{-/-}$ cross, this strongly suggests that IL-1α and IL-33 are in vivo necroptotic DAMPs in *Ripk1*$^{-/-}$ mice. Furthermore, because *Myd88*$^{-/-}$ mice are defective in IL-33 and IL-1α -mediated inflammatory signaling and *Myd88* deficiency extends the survival of *Ripk1*$^{-/-}$ mice, we conclude that these necroptotic DAMPs play a major role in the *Ripk1*$^{-/-}$ lethal systemic inflammation.

Our findings reveal an essential physiological role for RIPK1 in immune homeostasis and emergency hematopoiesis. Remarkably, direct regulation of TNFR1 by RIPK1 is not important to prevent inflammation or cell death in the embryo, except in a tissue-specific manner. RIPK1 is required for TNF-induced necroptosis at E10.5; however, surprisingly, in later stages of embryogenesis, RIPK1 plays an essential role in inhibiting necroptosis. The fact that the *Ripk1*$^{-/-}$*Mlkl*$^{-/-}$ mice phenocopy the *Ripk1*$^{-/-}$*Ripk3*$^{-/-}$ mice provides the strongest evidence so far that, in the context of inflammatory signaling, the role of RIPK3 in generating necroptotic DAMPs is at least as important as its direct role in promoting inflammatory cytokine production. We therefore propose that loss of RIPK1 inhibition of RIPK3/MLKL-dependent necroptosis promotes the production and release of necroptotic DAMPs such as IL-1α and IL-33, revealing a key function for RIPK1 in limiting, not only promoting, inflammation.

EXPERIMENTAL PROCEDURES

Mice

All mice were backcrossed to C57BL/6J mice for >10 generations or generated on a C57BL/6J background. *Mlkl*$^{-/-}$ mice were generated as described (Murphy et al., 2013). Mice obtained by Caesarean section at E19.5 or a few hours after natural birth were designated P0. Pregnant mice were prepared for Caesarean delivery by progesterone injection at E17.5 and E18.5. The relevant Animal Ethics Committee approved all experiments.

Histology and Immunofluorescence

Embryos were fixed in 10% neutral buffered formalin, paraffin embedded, and sectioned for routine histology staining (H&E). For skin immunofluorescence, paraffin sections were dewaxed, subjected to heat-induced epitope retrieval (HIER) with citrate buffer, blocked in 3% goat serum, permeabilized with 0.3% Triton X-100, and stained with keratin 6 (Covance), keratin 14, and goat anti-rabbit alexa-594 (Invitrogen) antibodies. Nuclei were visualized using Hoechst (Invitrogen). For tissue immunohistochemistry, sections were dewaxed and subjected to antigen retrieval in trypsin buffer (F4/80) or HIER with citrate buffer (CD45, CC3) and stained with the following antibodies: anti-CC3 (Cell Signaling Technology 9661), anti-CD45 (BD), anti-F4/80 (generated in-house), goat anti-rabbit biotinylated, and goat anti-rat biotinylated antibodies (Vector Laboratories). Images were taken using a DP72 microscope and cellSens Standard software (Olympus).

Cytokine Bioplex Assay

Cytokines were measured by Bioplex Pro mouse cytokine 23-plex assay (Bio-Rad) according to manufacturer's instructions. Where a value was above or below the reference range, it was assigned the value of the highest or lowest standard, respectively. Lysates were made by homogenizing organs in ice-cold protein DISC lysis buffer followed by protein level normalization using a BCA assay (Thermo Scientific). Skin samples were obtained from mice delivered by Caesarean at E20.5.

Chimeras

For hematopoietic reconstitution experiments, congenic C57BL/6.SJL (*Ptprc*^{a} *Pep3*^{b} [Ly5.1]) mice were reconstituted with 10^6 *Ptprc*^{b} *Pep3*^{a} (Ly5.2) fetal liver cells from E13.5 embryos. Serial transplants: 0.2–5 × 10^6 bone marrow cells

from primary donors were reconstituted into secondary irradiated Ly5.1 recipient mice. Competitive transplants: Ly5.1 mice were reconstituted with 10^6 fetal liver cells from Ly5.1/5.2 and knockout Ly5.2 mice at a 1:1 ratio. TNF-neutralization: mice were injected with 200 μg of anti-TNF (XT22) or isotype control three times per week for 2 weeks and then weekly for 6 weeks. Recipient mice received two 5.5-Gy doses of irradiation given 3 hr apart.

Progenitor Cell Analysis

Clonal cultures of hematopoietic cells were performed as described (Croker et al., 2004). For some experiments, sorted lineage$^-$ cKit$^+$ E18.5 liver cells were cultured in 100 ng/ml SCF + 10 ng/ml IL-3 + 4U/ml EPO with PBS, 10 ng/ml TNF, or 200 ng/ml Fc-FasL for 24 hr. To analyze progenitor viability, lineage$^-$ cKit$^+$ cells were monitored by flow cytometry with PI.

Immunoblotting

Organ lysates were made by homogenizing whole intestine or dorsal skin from P0 mice in ice-cold DISC lysis buffer containing cOmplete protease inhibitor cocktail (Roche), 20 μM MG132, 5 mM N-ethylmaleimide, 10 mM sodium fluoride, 5 mM β-glycerophosphate, 2 mM sodium pyrophosphate, 2 mM sodium pervanadate, and 1 mM sodium molybdate. Insoluble component was spun down, and supernatants were quantified with a BCA assay (Thermo Scientific). Supernatants were boiled with SDS reducing sample buffer. Plasma samples were diluted with PBS and boiled with SDS reducing sample buffer. Organ lysates and plasma samples were run on 4%–12% Bis-Tris gels (Invitrogen). Fetal liver lineage$^-$ cKit$^+$ cells were lysed as previously described (Croker et al., 2004). Membranes were probed with CC3 or -8 (Cell Signaling Technology 9661 and 8592, respectively), IL1α (Abcam ab9724), IL33 (R&D Systems AF3626), IL1β (R&D Systems AF-401-NA), caspase-1 (Santa Cruz sc-514 or clone 4G8; gift from Lorraine O'Reilly), MLKL (clone 3H1 described in Murphy et al. [2013]), RIPK1 (BD Transduction 610458), RIPK3 (Axxora PSC-2283-c100), cFLIP (ProScience XA-1008), HMGB1 (Abcam ab18256), or β-actin (Sigma-Aldrich A-1978) antibodies.

Hematology and Flow Cytometry

Automated cell counts were performed on blood collected from the retro-orbital plexus into Microtainer tubes containing EDTA (Sarstedt) using an Advia 2120 hematological analyzer (Siemens). For further analysis, blood smears were performed and assessed following May-Grünwald Giemsa staining. Flow cytometric analysis of hematopoietic cells was performed on a BD Biosciences LSRFortessa cell analyzer and analyzed using FlowJo software (Treestar). Ly5.1 and Ly5.2 expression determined the contribution of donor and recipient cells. Blood glucose was quantified using an Accu-Chek Performa (Roche) glucometer.

Bone-Marrow-Derived Macrophages and Fetal-Liver-Derived Macrophages

Macrophages were generated by culturing cell suspensions generated from bone marrow (for bone-marrow-derived macrophages, BMDMs) or E14.5 fetal livers (for fetal-liver-derived macrophages, FLDM) and differentiated for 7 days in M-CSF L929 conditioned media. For cell death assays, FLDMs were treated with recombinant human Fc-TNF and QVD (SM Biochemicals LLC) as indicated for 24 hr and then subjected to cell death analysis by flow cytometry quantification of PI uptake using a FACSCalibur (BD Biosciences). For the inflammasome assays, FLDMs were plated at 50–100,000 cells per well in a 96 well plate and stimulated with LPS (20 ng/ml) for 6–8 hr followed by ±5 mM ATP for 40–60 min. Lysates and supernatants were analyzed by western blotting. Supernatants were analyzed by ELISA (IL-1β, R&D Systems). Controls for caspase-1 and IL-1β detection in plasma and organs using western blotting were generated using BMDMs treated as above or pretreated with LPS for 2 hr followed by Smac mimetic treatment for 6 hr (GT12911, TetraLogic Pharmaceuticals). For Figure S6C, BMDMs of indicated genotypes (n = 3) were treated with LPS (20 ng/ml) for 9 hr, and IL-6 levels in supernatants were analyzed by ELISA (eBioscience).

Statistics

Unless otherwise specified, data are presented as mean + 1 SEM. Comparisons were performed with a Student's t test.

SUPPLEMENTAL INFORMATION

Supplemental Information includes seven figures and three tables and can be found with this article online at http://dx.doi.org/10.1016/j.cell.2014.04.019.

AUTHOR CONTRIBUTIONS

Phenotypic analysis was performed by J.A.R., J.A.O., J.M.E., and M.G. Mouse crosses were established by J.S., J.A.R., J.M.E., B.A.C., M.G., and J.A.O.; J.A.R. performed histological and immunohistological analysis with assistance from D.M., A.R.P. and H.A.; J.A.O., B.A.C., and M.G. performed hematopoietic progenitor analysis, transplant, and flow cytometry experiments. J.M.E., N.L., and M.G. performed plasma and tissue western blot analysis. Colony assays were performed by D.M. with assistance from L.D.R. and S.M.; J.E.V., K.E.L., M.G., and N.L. analyzed FLDM. All other experimental analysis was performed by J.A.R., J.A.O., J.M.E., and M.G. with assistance from H.A., R.L.N., C.H., S.K.S., T.J.P., L.H.C., J.C., and S.M.; T.R. performed anatomical pathology analysis. W.S.A., J.M.M., M.E., G.D., D.L.V., S.L.M., P.G.E., H.E.A., and A.W.R. provided reagents and advice and assisted with interpretation of experiments. W.S.A. and J.M.M. generated *Mlkl*$^{-/-}$ mice. J.S., M.G., B.A.C., J.A.R., J.A.O., and J.M.E. conceived and coordinated the project, interpreted results, and wrote the manuscript.

ACKNOWLEDGMENTS

We thank staff in the WEHI Bioservices facility, Vishva Dixit for *Ripk3*$^{-/-}$ mice, Michelle Kelliher for *Ripk1*$^{-/-}$ mice, Heinrich Korner for *Tnf*$^{-/-}$ and *Tnfr1*$^{-/-}$ mice, Stephen Hedrick for *Casp8*$^{fl/fl}$ mice, and Anne Voss for helpful discussions. This work was supported by NHMRC grants (1016647, 461221, 1016701, 1025594, 1046984, 1046010, 1025239, 637367, 1008131, and 1057905), an Australian Research Council Fellowship (B.A.C.), an APA scholarship (J.A.R.), a Dora Lush Scholarship (J.A.O.), a La Trobe University Postgraduate Research Scholarship (J.M.E.), a VESKI innovation fellowship (S.L.M.), ARC Fellowship (J.M.M.), Cancer Council Victoria Carden Fellowship (D.M.), and NHMRC fellowships to J.S., W.S.A., and A.W.R. (541901, 1058344, and 637309) with additional support from the Australian Cancer Research Fund, Victorian State Government Operational Infrastructure Support, and an NHMRC IRIISS grant (361646).

Received: October 30, 2013
Revised: March 28, 2014
Accepted: April 14, 2014
Published: May 8, 2014

REFERENCES

Beutler, B., Jiang, Z., Georgel, P., Crozat, K., Croker, B., Rutschmann, S., Du, X., and Hoebe, K. (2006). Genetic analysis of host resistance: Toll-like receptor signaling and immunity at large. Annu. Rev. Immunol. *24*, 353–389.

Bonnet, M.C., Preukschat, D., Welz, P.S., van Loo, G., Ermolaeva, M.A., Bloch, W., Haase, I., and Pasparakis, M. (2011). The adaptor protein FADD protects epidermal keratinocytes from necroptosis in vivo and prevents skin inflammation. Immunity *35*, 572–582.

Chen, X., Li, W., Ren, J., Huang, D., He, W.T., Song, Y., Yang, C., Li, W., Zheng, X., Chen, P., et al. (2014). Translocation of mixed lineage kinase domain-like protein to plasma membrane leads to necrotic cell death. Cell Res. *24*, 105–121.

Cohen, I., Rider, P., Carmi, Y., Braiman, A., Dotan, S., White, M.R., Voronov, E., Martin, M.U., Dinarello, C.A., and Apte, R.N. (2010). Differential release of chromatin-bound IL-1α discriminates between necrotic and apoptotic cell death by the ability to induce sterile inflammation. Proc. Natl. Acad. Sci. USA *107*, 2574–2579.

Croker, B.A., Metcalf, D., Robb, L., Wei, W., Mifsud, S., DiRago, L., Cluse, L.A., Sutherland, K.D., Hartley, L., Williams, E., et al. (2004). SOCS3 is a critical physiological negative regulator of G-CSF signaling and emergency granulopoiesis. Immunity *20*, 153–165.

Cusson, N., Oikemus, S., Kilpatrick, E.D., Cunningham, L., and Kelliher, M. (2002). The death domain kinase RIP protects thymocytes from tumor necrosis factor receptor type 2-induced cell death. J. Exp. Med. *196*, 15–26.

Dillon, C.P., Oberst, A., Weinlich, R., Janke, L.J., Kang, T.B., Ben-Moshe, T., Mak, T.W., Wallach, D., and Green, D.R. (2012). Survival function of the FADD-CASPASE-8-cFLIP(L) complex. Cell Rep. *1*, 401–407.

Dillon, C.P., Weinlich, R., Rodriguez, D.A., Cripps, J.G., Quarato, G., Gurung, P., Verbist, K.C., Brewer, T.L., Llambi, F., Gong, Y.-N., et al. (2014). RIPK1 blocks early postnatal lethality mediated by caspase-8 and RIPK3. Cell *157*, this issue, 1189–1202.

Ea, C.K., Deng, L., Xia, Z.P., Pineda, G., and Chen, Z.J. (2006). Activation of IKK by TNFalpha requires site-specific ubiquitination of RIP1 and polyubiquitin binding by NEMO. Mol. Cell *22*, 245–257.

Feoktistova, M., Geserick, P., Kellert, B., Dimitrova, D.P., Langlais, C., Hupe, M., Cain, K., MacFarlane, M., Häcker, G., and Leverkus, M. (2011). cIAPs block Ripoptosome formation, a RIP1/caspase-8 containing intracellular cell death complex differentially regulated by cFLIP isoforms. Mol. Cell *43*, 449–463.

Gentle, I.E., Wong, W.W., Evans, J.M., Bankovacki, A., Cook, W.D., Khan, N.R., Nachbur, U., Rickard, J., Anderton, H., Moulin, M., et al. (2011). In TNF-stimulated cells, RIPK1 promotes cell survival by stabilizing TRAF2 and cIAP1, which limits induction of non-canonical NF-kappaB and activation of caspase-8. J. Biol. Chem. *286*, 13282–13291.

Gerlach, B., Cordier, S.M., Schmukle, A.C., Emmerich, C.H., Rieser, E., Haas, T.L., Webb, A.I., Rickard, J.A., Anderton, H., Wong, W.W., et al. (2011). Linear ubiquitination prevents inflammation and regulates immune signalling. Nature *471*, 591–596.

Kaczmarek, A., Vandenabeele, P., and Krysko, D.V. (2013). Necroptosis: the release of damage-associated molecular patterns and its physiological relevance. Immunity *38*, 209–223.

Kaiser, W.J., Upton, J.W., Long, A.B., Livingston-Rosanoff, D., Daley-Bauer, L.P., Hakem, R., Caspary, T., and Mocarski, E.S. (2011). RIP3 mediates the embryonic lethality of caspase-8-deficient mice. Nature *471*, 368–372.

Kaiser, W.J., Sridharan, H., Huang, C., Mandal, P., Upton, J.W., Gough, P.J., Sehon, C.A., Marquis, R.W., Bertin, J., and Mocarski, E.S. (2013). Toll-like receptor 3-mediated necrosis via TRIF, RIP3, and MLKL. J. Biol. Chem. *288*, 31268–31279.

Kang, T.B., Ben-Moshe, T., Varfolomeev, E.E., Pewzner-Jung, Y., Yogev, N., Jurewicz, A., Waisman, A., Brenner, O., Haffner, R., Gustafsson, E., et al. (2004). Caspase-8 serves both apoptotic and nonapoptotic roles. J. Immunol. *173*, 2976–2984.

Kang, T.B., Yang, S.H., Toth, B., Kovalenko, A., and Wallach, D. (2013). Caspase-8 blocks kinase RIPK3-mediated activation of the NLRP3 inflammasome. Immunity *38*, 27–40.

Kayagaki, N., Warming, S., Lamkanfi, M., Vande Walle, L., Louie, S., Dong, J., Newton, K., Qu, Y., Liu, J., Heldens, S., et al. (2011). Non-canonical inflammasome activation targets caspase-11. Nature *479*, 117–121.

Kelliher, M.A., Grimm, S., Ishida, Y., Kuo, F., Stanger, B.Z., and Leder, P. (1998). The death domain kinase RIP mediates the TNF-induced NF-kappaB signal. Immunity *8*, 297–303.

Korner, H., Cook, M., Riminton, D.S., Lemckert, F.A., Hoek, R.M., Ledermann, B., Kontgen, F., Fazekas de St Groth, B., and Sedgwick, J.D. (1997). Distinct roles for lymphotoxin-alpha and tumor necrosis factor in organogenesis and spatial organization of lymphoid tissue. Eur. J. Immunol. *27*, 2600–2609.

Lefrançais, E., Roga, S., Gautier, V., Gonzalez-de-Peredo, A., Monsarrat, B., Girard, J.P., and Cayrol, C. (2012). IL-33 is processed into mature bioactive forms by neutrophil elastase and cathepsin G. Proc. Natl. Acad. Sci. USA *109*, 1673–1678.

Lüthi, A.U., Cullen, S.P., McNeela, E.A., Duriez, P.J., Afonina, I.S., Sheridan, C., Brumatti, G., Taylor, R.C., Kersse, K., Vandenabeele, P., et al. (2009). Suppression of interleukin-33 bioactivity through proteolysis by apoptotic caspases. Immunity *31*, 84–98.

Meylan, E., Burns, K., Hofmann, K., Blancheteau, V., Martinon, F., Kelliher, M., and Tschopp, J. (2004). RIP1 is an essential mediator of Toll-like receptor 3-induced NF-κ B activation. Nat. Immunol. *5*, 503–507.

Michallet, M.C., Meylan, E., Ermolaeva, M.A., Vazquez, J., Rebsamen, M., Curran, J., Poeck, H., Bscheider, M., Hartmann, G., König, M., et al. (2008). TRADD protein is an essential component of the RIG-like helicase antiviral pathway. Immunity *28*, 651–661.

Micheau, O., and Tschopp, J. (2003). Induction of TNF receptor I-mediated apoptosis via two sequential signaling complexes. Cell *114*, 181–190.

Micheau, O., Lens, S., Gaide, O., Alevizopoulos, K., and Tschopp, J. (2001). NF-kappaB signals induce the expression of c-FLIP. Mol. Cell. Biol. *21*, 5299–5305.

Moujalled, D.M., Cook, W.D., Okamoto, T., Murphy, J., Lawlor, K.E., Vince, J.E., and Vaux, D.L. (2013). TNF can activate RIPK3 and cause programmed necrosis in the absence of RIPK1. Cell Death Dis. *4*, e465.

Murphy, J.M., Czabotar, P.E., Hildebrand, J.M., Lucet, I.S., Zhang, J.G., Alvarez-Diaz, S., Lewis, R., Lalaoui, N., Metcalf, D., Webb, A.I., et al. (2013). The pseudokinase MLKL mediates necroptosis via a molecular switch mechanism. Immunity *39*, 443–453.

Oberst, A., Dillon, C.P., Weinlich, R., McCormick, L.L., Fitzgerald, P., Pop, C., Hakem, R., Salvesen, G.S., and Green, D.R. (2011). Catalytic activity of the caspase-8-FLIP(L) complex inhibits RIPK3-dependent necrosis. Nature *471*, 363–367.

Panayotova-Dimitrova, D., Feoktistova, M., Ploesser, M., Kellert, B., Hupe, M., Horn, S., Makarov, R., Jensen, F., Porubsky, S., Schmieder, A., et al. (2013). cFLIP regulates skin homeostasis and protects against TNF-induced keratinocyte apoptosis. Cell Rep. *5*, 397–408.

Pasparakis, M., Courtois, G., Hafner, M., Schmidt-Supprian, M., Nenci, A., Toksoy, A., Krampert, M., Goebeler, M., Gillitzer, R., Israel, A., et al. (2002). TNF-mediated inflammatory skin disease in mice with epidermis-specific deletion of IKK2. Nature *417*, 861–866.

Pearl-Yafe, M., Mizrahi, K., Stein, J., Yolcu, E.S., Kaplan, O., Shirwan, H., Yaniv, I., and Askenasy, N. (2010). Tumor necrosis factor receptors support murine hematopoietic progenitor function in the early stages of engraftment. Stem Cells *28*, 1270–1280.

Piao, X., Komazawa-Sakon, S., Nishina, T., Koike, M., Piao, J.H., Ehlken, H., Kurihara, H., Hara, M., Van Rooijen, N., Schütz, G., et al. (2012). c-FLIP maintains tissue homeostasis by preventing apoptosis and programmed necrosis. Sci. Signal. *5*, ra93.

Scaffidi, P., Misteli, T., and Bianchi, M.E. (2002). Release of chromatin protein HMGB1 by necrotic cells triggers inflammation. Nature *418*, 191–195.

Schmukle, A.C., and Walczak, H. (2012). No one can whistle a symphony alone - how different ubiquitin linkages cooperate to orchestrate NF-κB activity. J. Cell Sci. *125*, 549–559.

Sun, L., Wang, H., Wang, Z., He, S., Chen, S., Liao, D., Wang, L., Yan, J., Liu, W., Lei, X., et al. (2012). Mixed lineage kinase domain-like protein mediates necrosis signaling downstream of RIP3 kinase. Cell *148*, 213–227.

Upton, J.W., Kaiser, W.J., and Mocarski, E.S. (2010). Virus inhibition of RIP3-dependent necrosis. Cell Host Microbe *7*, 302–313.

Vandenabeele, P., Galluzzi, L., Vanden Berghe, T., and Kroemer, G. (2010). Molecular mechanisms of necroptosis: an ordered cellular explosion. Nat. Rev. Mol. Cell Biol. *11*, 700–714.

Varfolomeev, E.E., Schuchmann, M., Luria, V., Chiannilkulchai, N., Beckmann, J.S., Mett, I.L., Rebrikov, D., Brodianski, V.M., Kemper, O.C., Kollet, O., et al. (1998). Targeted disruption of the mouse Caspase 8 gene ablates cell death induction by the TNF receptors, Fas/Apo1, and DR3 and is lethal prenatally. Immunity *9*, 267–276.

Vince, J.E., Wong, W.W., Gentle, I., Lawlor, K.E., Allam, R., O'Reilly, L., Mason, K., Gross, O., Ma, S., Guarda, G., et al. (2012). Inhibitor of apoptosis proteins limit RIP3 kinase-dependent interleukin-1 activation. Immunity *36*, 215–227.

Weill, D., Gay, F., Tovey, M.G., and Chouaib, S. (1996). Induction of tumor necrosis factor alpha expression in human T lymphocytes following ionizing gamma irradiation. J. Interferon Cytokine Res. *16*, 395–402.

Wertz, I.E., and Dixit, V.M. (2010). Regulation of death receptor signaling by the ubiquitin system. Cell Death Differ. *17*, 14–24.

Wong, W.W., Vince, J.E., Lalaoui, N., Lawlor, K.E., Chau, D., Bankovacki, A., Anderton, H., Metcalf, D., O'Reilly, L., Jost, P.J., et al. (2014). cIAPs and XIAP regulate myelopoiesis through cytokine production in an RIPK1- and RIPK3-dependent manner. Blood *123*, 2562–2572.

Yeh, W.C., de la Pompa, J.L., McCurrach, M.E., Shu, H.B., Elia, A.J., Shahinian, A., Ng, M., Wakeham, A., Khoo, W., Mitchell, K., et al. (1998). FADD: essential for embryo development and signaling from some, but not all, inducers of apoptosis. Science *279*, 1954–1958.

Yeh, W.C., Itie, A., Elia, A.J., Ng, M., Shu, H.B., Wakeham, A., Mirtsos, C., Suzuki, N., Bonnard, M., Goeddel, D.V., and Mak, T.W. (2000). Requirement for Casper (c-FLIP) in regulation of death receptor-induced apoptosis and embryonic development. Immunity *12*, 633–642.

Zhao, J., Jitkaew, S., Cai, Z., Choksi, S., Li, Q., Luo, J., and Liu, Z.G. (2012). Mixed lineage kinase domain-like is a key receptor interacting protein 3 downstream component of TNF-induced necrosis. Proc. Natl. Acad. Sci. USA *109*, 5322–5327.